J|A|C|S
ARTICLES
Published on Web 05/17/2006

Self-Assembled π-Nanotapes as Donor Scaffolds for Selective and Thermally Gated Fluorescence Resonance Energy Transfer (FRET)

Vakayil K. Praveen, Subi J. George, Reji Varghese, Chakkooth Vijayakumar, and Ayyappanpillai Ajayaghosh*

Contribution from the Photosciences and Photonics Group, Chemical Sciences and Technology Division, Regional Research Laboratory, CSIR, Trivandrum 695 019, India

Received December 26, 2005; E-mail: aajayaghosh@rediffmail.com

Abstract: Self-assembled nanotapes of a few tailor-made oligo(*p*-phenylenevinylene)s (OPVs) have been prepared and used as supramolecular donor scaffold to study the fluorescence resonance energy transfer (FRET) to a suitable acceptor. In nonpolar solvents, FRET occurs with nearly 63−81% efficiency, exclusively from the self-assembled OPVs to entrapped Rhodamine B, resulting in the quenching of the donor emission with concomitant formation of the acceptor emission at 625 nm. The efficiency of FRET is considerably influenced by the ability of the OPVs to form the self-assembled aggregates and hence could be controlled by structural variation of the molecules, and polarity of the solvent. Most importantly, FRET could be controlled by temperature as a result of the thermally reversible self-assembly process. The FRET efficiency was significantly enhanced (ca. 90%) in a xerogel film of the **OPV1** which is dispersed with relatively less amount of the acceptor (33 mol %), when compared to that of the aggregates in dodecane gel. FRET is not efficient in polar solvents due to weak self-organization of the chromophores. These results indicate that energy transfer occurs exclusively from the self-assembled donor and not directly from the individual donor molecules. The present study illustrates that the self-assembly of chromophores facilitates temperature and solvent controlled FRET within π-conjugated nanostructures.

Introduction

Photoinduced energy transfer is one of the fundamental processes of natural photosynthetic systems and has been a subject of numerous studies. Supramolecular organization of chromophores[1] play crucial role in facilitating energy and electron-transfer processes in natural light harvesting assemblies.[2] On the other hand, these processes have become extremely important in the field of organic based optoelectronic materials,[3] particularly in the emerging field of supramolecular electronics.[4] Among several strategies adopted for chromophore organization, the use of H-bonded supramolecular assemblies need special mention in the context of the present work.[5] In recent years, a number of H-bonded donor−acceptor systems have been reported for energy transfer studies in which the self-assembly is restricted to the formation of dimeric or trimeric complexes.[6,7] Therefore, creation of higher order supramolecular assemblies of nano- to micrometer length scale is important when electron or energy transport processes are addressed. In this context, energy transfer within chromophore based organogelators has been of great interest in recent times.[8−10]

(1) For recent reviews of supramolecular organization of chromophores, see: (a) Hoeben, F. J. M.; Jonkheijm, P.; Meijer, E. W.; Schenning, A. P. H. J. *Chem. Rev.* **2005**, *105*, 1491−1546. (b) *Supramolecular Dye Chemistry*; Würthner, F.; Ed.; *Top. Curr. Chem.*: Springer-Verlag: Berlin, Heidelberg, **2005**, *258*, 1−324.

(2) (a) Kühlbrandt, W.; Wang, D. N. *Nature (London)* **1991**, *350*, 130−134. (b) Kühlbrandt, W. *Nature (London)* **1995**, *374*, 497−498. (c) McDermott, G.; Prince, S. M.; Freer, A. A.; Hawthornthwaite-Lawless, A. M.; Papiz, M. Z.; Cogdell, R. J.; Isaacs, N. W. *Nature* **1995**, *374*, 517−521.

(3) For reviews, see: (a) Carroll, R. L.; Gorman, C. B. *Angew. Chem., Int. Ed.* **2002**, *41*, 4378−4400. (b) Forrest, S. R. *Nature (London)* **2004**, *428*, 911−918. (c) Grimsdale, A. C.; Müllen, K. *Angew. Chem., Int. Ed.* **2005**, *44*, 5592−5629.

(4) (a) Meijer, E. W.; Schenning, A. P. H. J. *Nature (London)* **2002**, *419*, 353−354. (b) Van Der Auweraer, M.; De Schryver, F. C. *Nat. Mater.* **2004**, *3*, 507−508. (c) Schenning, A. P. H. J.; Meijer, E. W. *Chem. Commun.* **2005**, 3245−3258.

(5) Ajayaghosh, A.; George, S. J.; Schenning, A. P. H. J. *Top. Curr. Chem.* **2005**, *258*, 83−118, and references therein.

(6) For reviews on H-bonded assemblies based energy transfer systems, see: (a) Ward, M. D. *Chem. Soc.* Rev. **1997**, *26*, 365−375 (b) Sánchez, L. S.; Martín, N.; Guldi, D. M. *Angew. Chem., Int. Ed.* **2005**, *44*, 5374−5382.

(7) (a) Encinas, S.; Simpson, N. R. M.; Andrews, P.; Ward, M. D.; White, C. M.; Armaroli, N.; Barigelletti, F.; Houlton, A. *New J. Chem.* **2000**, *24*, 987−991. (b) Rau, S.; Schäfer, B.; Schebesta, S.; Grüssing, A.; Poppitz, W.; Walther, D.; Duati, M.; Browne, W. R.; Vos, J. G. *Eur. J. Inorg. Chem.* **2003,** 1503−1506. (c) Otsuki, J.; Iwasaki, K.; Nakano, Y.; Itou, M.; Araki, Y.; Ito, O. *Chem. Eur. J.* **2004**, *10*, 3461−3466.

(8) For reviews of low molecular weight organogels, see: (a) Terech, P.; Weiss, R. G. *Chem. Rev.* **1997**, *97*, 3133−3159. (b) van Esch, J. H.; Feringa, B. L. *Angew. Chem., Int. Ed.* **2000**, *39*, 2263−2266. (c) Sangeetha, N. M.; Maitra, U. *Chem. Soc. Rev.* **2005**, *34*, 821−836. (d) *Molecular Gels, Materials with Self-Assembled Fibrillar Networks*; Terech, P., Weiss, R. G., Eds.; Kluwer Press: Dordrecht, The Netherlands, 2005.

(9) For light harvesting organogels, see: (a) Sagawa, T.; Fukugawa, S.; Yamada, T.; Ihara, H. *Langmuir* **2002**, *18*, 7223−7228. (b) Nakashima, T.; Kimizuka, N. *Adv. Mater.* **2002**, *14*, 1113−1116. (c) Sugiyasu, K.; Fujita, N.; Takeuchi, M.; Yamada, S.; Shinkai, S. *Org. Biomol. Chem.* **2003**, *1*, 895−899.

(10) (a) Sugiyasu, K.; Fujita, N.; Shinkai, S. *Angew. Chem., Int. Ed.* **2004**, *43*, 1229−1233. (b) Ryu, J.-H.; Lee, M. *J. Am. Chem. Soc.* **2005**, *127*, 14170−14171. (c) Yamaguchi, S.; Yoshimura, I.; Kohira, T.; Tamaru, S.-i.; Hamachi, I. *J. Am. Chem. Soc.* **2005**, *127*, 11835−11841. (d) Del Guerzo, A.; Olive, A. G. L.; Reichwagen, J.; Hopf, H.; Desvergne, J.-P. *J. Am. Chem. Soc.* **2005**, *127*, 17984−17985. (e) Montalti, M.; Dolci, L. S.; Prodi, L.; Zaccheroni, N.; Stuart, M. C. A.; van Bommel, K. J. C.; Friggeri, A. *Langmuir* **2006**, *22*, 2299−2303.

10.1021/ja0587594 CCC: $33.50

Chart 1. Molecular Structures of the OPV Donors and the Acceptor under Investigation.

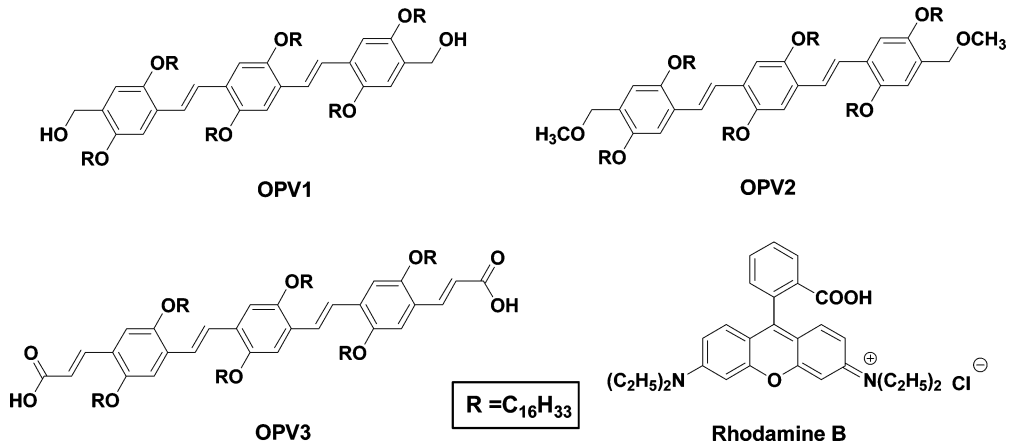

Scheme 1

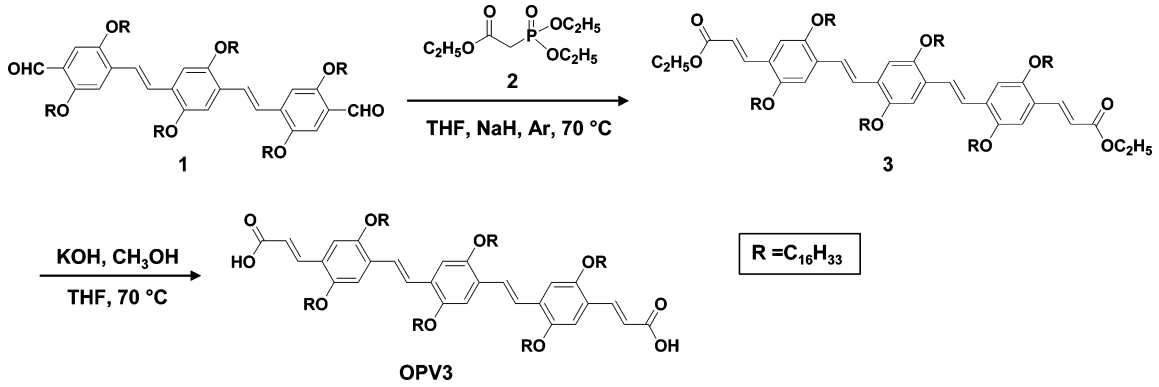

Linear π-conjugated systems, particularly oligo(*p*-phenylenevinylene)s (OPVs) are known to be efficient energy donors to different acceptors. For example, Heeger, Bazan, Swager, Schanze, and others have shown fluorescence resonance energy transfer (FRET) from functionalized linear π-conjugated systems to suitable acceptors.[11−18] The research groups of Meijer, Janssen and Würthner have extensively studied the energy transfer processes in quadruple H-bonded OPV self-assemblies[19,20] and OPV-perylene bisimide coassemblies.[21,22] The intension of the present study is to demonstrate the use of supramolecular architectures and organogels of OPVs as energy donor scaffolds for FRET. OPVs which are functionalized with H-bonding groups and long alkyl side chains form stable organogels with good optical properties.[23,24] After our report on OPV based π-gels,[23a] Stupp and co-workers have shown the gelation of asymmetrically end-substituted OPV based amphiphiles.[25] In the above cases, the emission of OPVs exhibit significant shift toward long wavelength region as a result of gelation.[23c] This property of self-assembled OPVs make them ideal energy donor scaffolds to suitable acceptors that facilitate FRET processes.[26] Herein, we report the detailed investigation on the use of a few OPV self-assemblies as FRET donors to an entrapped organic dye (Rhodamine B).[27]

Results and Discussion

The structures of the donors and the acceptor under investigation are shown in Chart 1. **OPV1** and **OPV2** were prepared as per reported procedures.[23c] **OPV3** was synthesized as per Scheme 1. The optical properties of these molecules exhibit significant changes in different solvents (Table 1). The thermoreversible shift of the absorption and the emission bands indicate the aggregation of the molecules in cyclohexane and in dodecane.[23c] Thermal stability of the self-assembly is strongly dependent upon the end functional groups of the OPVs. Plots of the fraction of aggregates (α) vs temperature (Figure 1) exhibit sigmoidal type transitions within short temperature range in the case of **OPV1** and **OPV2**, which indicate a cooperative self-assembly process.[19d,28] However, in the case of **OPV3** a broad transition is obtained for a wide temperature range. The carboxylic acid groups of **OPV3** participate in two-point linear H-bonding interactions leading to the formation of one-dimensional supramolecular polymeric aggregate. They subsequently undergo π-stacking, resulting in higher order structures

(11) (a) Stork, M.; Gaylord, B. S.; Heeger, A. J.; Bazan, G. C. *Adv. Mater.* **2002**, *14*, 361−366. (b) Gaylord, B. S.; Heeger, A. J.; Bazan, G. C. *J. Am. Chem. Soc.* **2003**, *125*, 896−900. (c) Liu, B.; Gaylord, B. S.; Wang, S.; Bazan, G. C. *J. Am. Chem. Soc.* **2003**, *125*, 6705−6714. (d) Wang, S.; Gaylord, B. S.; Bazan, G. C. *J. Am.* Chem. Soc. **2004**, *126*, 5446−5451. (e) Liu, B.; Bazan, G. C. *J. Am. Chem. Soc.* **2006**, *128*, 1188−1196.
(12) (a) McQuade, D. T.; Hegedus, A. H.; Swager, T. M. *J. Am. Chem. Soc.* **2000**, *122*, 12389−12390. (b) Zheng, J.; Swager, T. M. *Chem. Commun.* **2004**, 2798−2799. (c) Kuroda, K.; Swager, T. M. *Macromolecules* **2004**, *37*, 716−724.
(13) (a) Tan, C.; Atas, E.; Müller, J. G.; Pinto, M. R.; Kleiman, V. D.; Schanze, K. S. *J. Am. Chem. Soc.* **2004**, *126*, 13685−13694. (b) Müller, J. G.; Atas, E.; Tan, C.; Schanze, K. S.; Klieman, V. D. *J. Am. Chem. Soc.* **2006**, *128*, 4007−4016.
(14) (a) Cheng, Y.-J.; Hwu, T.-Y.; Hsu, J.-H.; Luh, T.-Y. *Chem. Commun.* **2002**, 1978−1979. (b) Chen, C.-H.; Liu, K.-Y.; Sudhakar, S.; Lim, T.-S.; Fann, W.; Hsu, C.-P.; Luh, T.-Y. *J. Phys. Chem. B* **2005**, *109*, 17887−17891.
(15) (a) Armaroli, N.; Accorsi, G.; Rio, Y.; Nierengarten, J.-F.; Eckert, J.-F.; Gómez-Escalonilla, M. J.; Langa, F. *Synth. Met.* **2004**, *147*, 19−28, and references therein. (b) Gutierrez-Nava, M.; Accorsi, G.; Masson, P.; Armaroli, N.; Nierengarten, J.-F. *Chem.-Eur. J.* **2004**, *10*, 5076−5086. (c) Langa, F.; Gómez-Escalonilla, M. J.; Rueff, J.-M.; Duarte, T. M. F.; Nierengarten, J.-F.; Palermo, V.; Samorì, P.; Rio, Y.; Accorsi, G.; Armaroli, N. *Chem.-Eur. J.* **2005**, *11*, 4405−4415.

Table 1. Optical Properties and Energy Transfer Efficiencies of **OPV1-3**.

compd	solvent	absorption λ_{max} (nm)	emission λ_{max} (nm)	Φ_f	energy transfer efficiency (%)
OPV1	chloroform	407	463, 490	0.73[a]	
	cyclohexane	401, 468	454, 476, 527, 561	0.20[b]	63[c]
	dodecane	404, 467	537, 567	0.23[b]	72[d]
OPV2	chloroform	408	464, 496, 533	0.71[a]	
	cyclohexane	401	452, 480, 520	0.66[a]	10[c]
	dodecane	394, 465	517, 552	0.34[b]	63[d]
OPV3	chloroform	448	534, 562	0.90[b]	
	cyclohexane	470, 515	508, 545	0.69[b]	
	dodecane	475, 517	588	0.21[b]	81[d]

[a] Fluorescence quantum yields were determined using quinine sulfate as the standard ($\Phi_f = 0.546$ in 0.1 N H_2SO_4), ±5% error. [b] Fluorescence quantum yields were determined using Rhodamine 6G ($\Phi_f = 0.9$ in ethanol), ±5% error. [c] In cyclohexane-chloroform (16:1). [d] In dodecane-chloroform (16:1).

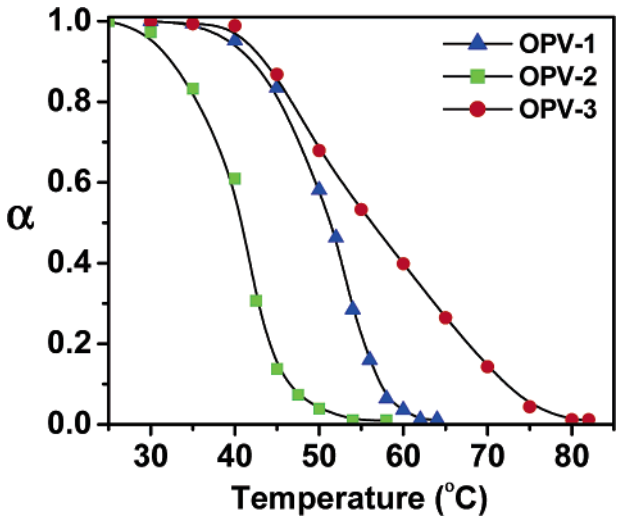

Figure 1. Stability of the OPV self-assemblies (1×10^{-5} M) in dodecane obtained from plots of aggregate fraction (α) vs temperature. The data points were obtained from the variable temperature absorption spectral changes at 470 nm (**OPV1**), 465 nm (**OPV2**) and 517 nm for **OPV3**.

that show better stability than the self-assemblies of **OPV1** and **OPV2**. These polymeric aggregates break at relatively higher temperatures in a noncooperative way as evident from the aggregate to monomer transition curve which could be the reason for the broad transition in Figure 1.[19d]

We have chosen Rhodamine B for the FRET studies since it is known to be a good energy acceptor from excited OPVs.[18a] The emission spectra of **OPV1**−**3** in cyclohexane or dodecane showed significant overlap with the absorption spectrum of Rhodamine B.[29] The absorption spectra of **OPV1-3** (1.01×10^{-5} M) in the presence of Rhodamine B (8.38×10^{-5} M) in cyclohexane-chloroform (16:1) revealed the absence of any ground-state interaction between the donor and the acceptor molecules. The fluorescence spectra of **OPV1** (1.01×10^{-5} M) in cyclohexane-chloroform (16:1) showed a broad emission corresponding to both monomeric and self-assembled species, when excited at 380 nm (Figure 2a). In the presence of Rhodamine B, the emission between 500 and 650 nm corresponding to the self-assembled **OPV1** is selectively quenched (ca. 63%) with concomitant emission at 625 nm, indicating the occurrence of FRET from the self-assembled donors. The emission between 400 and 480 nm of the molecularly dissolved OPVs was virtually unaffected indicating that FRET is not feasible from the unassembled OPVs. Direct excitation of a solution of Rhodamine B (8.38×10^{-5} M) at 380 nm in the absence of OPVs showed a negligible fluorescence at 625 nm. When the self-assembled species were selectively excited at 470 nm in the presence of Rhodamine B, 63% quenching of the **OPV1** emission could be observed (Figure 2b). The inset of Figure 2a shows a comparison of the emission of optically matching solutions of Rhodamine B upon direct ($\lambda_{ex} = 535$ nm) excitation with that of indirect excitation ($\lambda_{ex} = 470$ nm) in the presence of OPV nanotapes. The enhanced dye emission on indirect excitation when compared to that of the direct excitation indicates that the fluorescence quenching is not due to a trivial energy transfer but due to FRET from the OPV self-assembly to Rhodamine B.[11d,12a,30] FRET from the self-assembled OPVs

(16) (a) Guldi, D. M.; Swartz, A.; Luo, C.; Gómez, R.; Segura, J. L.; Martín, N. *J. Am. Chem. Soc.* **2002**, *124*, 10875−10886. (b) Giacalone, F.; Segura, J. L.; Martín, N.; Ramey, J.; Guldi, D. M. *Chem.-Eur. J.* **2005**, *11*, 4819−4834.
(17) (a) van Hal, P. A.; Janssen, R. A. J.; Lanzani, G.; Cerullo, G.; Zavelani-Rossi, M.; De Silvestri, S. *Phys. Rev. B* **2001**, *64*, 075206/1−075206/7. (b) Ramos, A. M.; Meskers, S. C. J.; van Hal, P. A.; Knol, J.; Hummelen, J. C.; Janssen, R. A. J. *J. Phys. Chem. A* **2003**, *107*, 9269−9283.
(18) (a) Schenning, A. P. H. J.; Peeters, E.; Meijer, E. W. *J. Am. Chem. Soc.* **2000**, *122*, 4489−4495. (b) Wolffs, M.; Hoeben, F. J. M.; Beckers, E. H. A.; Schenning, A. P. H. J.; Meijer, E. W. *J. Am. Chem. Soc.* **2005**, *127*, 13484−13485.
(19) For OPV H-bonded energy transfer systems. (a) Hoeben, F. J. M.; Herz, L. M.; Daniel, C.; Jonkheijm, P.; Schenning, A. P. H. J.; Silva, C.; Meskers, S. C. J.; Beljonne, D.; Phillips, R. T.; Friend, R. H.; Meijer, E. W. *Angew. Chem., Int. Ed.* **2004**, *43*, 1976−1979. (b) Daniel, C.; Herz, L. M.; Beljonne, D.; Hoeben, F. J. M.; Jonkheijm, P.; Schenning, A. P. H. J.; Meijer, E. W.; Phillips, R. T.; Silva, C. *Synth. Met.* **2004**, *147*, 29−35. (c) Beljone, D.; Hennebicq, E.; Daniel, C.; Herz, L. M.; Silva, C.; Scholes, G. D.; Hoeben, F. J. M.; Jonkheijm, P.; Schenning, A. P. H. J.; Meskers, S. C. J.; Phillips, R. T.; Friend, R. H.; Meijer, E. W. *J. Phys. Chem. B* **2005**, *109*, 10594−10604. (d) Hoeben, F. J. M.; Schenning, A. P. H. J.; Meijer, E. W. *Chem. Phys. Chem.* **2005**, *6*, 2337−2342.
(20) (a) Beckers, E. H. A.; Schenning, A. P. H. J.; van Hal, P. A.; El-ghayoury, A.; Sánchez, L.; Hummelen, J. C.; Meijer, E. W.; Janssen, R. A. J. *Chem. Commun.* **2002**, 2888−2889. (b) Beckers, E. H. A.; van Hal, P. A.; Schenning, A. P. H. J.; El-ghayoury, A.; Peeters, E.; Rispens, M. T.; Hummelen, J. C.; Meijer, E. W.; Janssen, R. A. J. *J. Mater. Chem.* **2002**, *12*, 2054−2060.
(21) For OPV-perylene bisimide systems. (a) Neuteboom, E. E.; Beckers, E. H. A.; Meskers, S. C. J.; Meijer, E. W.; Janssen, R. A. J. *Org. Biomol. Chem.* **2003**, *1*, 198−203. (b) Würthner, F.; Chen, Z.; Hoeben, F. J. M.; Osswald, P.; You, C.-C.; Jonkheijm, P.; van Herrikhuyzen, J.; Schenning, A. P. H. J.; van der Schoot, P. P. A. M.; Meijer, E. W.; Beckers, E. H. A.; Meskers, S. C. J.; Janssen, R. A. J. *J. Am. Chem. Soc.* **2004**, *126*, 10611−10618. (c) Dudek, S. P.; Pouderoijen, M.; Abbel, R.; Schenning, A. P. H. J.; Meijer, E. W. *J. Am. Chem.* Soc. **2005**, *127*, 11763−11768.
(22) (a) Neuteboom, E. E.; Meskers, S. C. J.; van Hal, P. A.; van Duren, J. K. J.; Meijer, E. W.; Janssen, R. A. J.; Dupin, H.; Pourtois, G.; Cornil, J.; Lazzaroni, R.; Brédas, J.-L.; Beljonne, D. *J. Am. Chem. Soc.*. **2003**, *125*, 8625−8638. (b) Neuteboom, E. E.; van Hal, P. A.; Janssen, R. A. J. *Chem.-Eur. J.* **2004**, *10*, 3907−3918. (c) Würthner, F. *Chem. Commun.* **2004**, 1564−1579. (d) Ramos, A. M.; Meskers, S. C. J.; Beckers, E. H. A.; Prince, R. B.; Brunsveld, L.; Janssen, R. A. J. *J. Am. Chem. Soc.* **2004**, *126*, 9630−9644.
(23) (a) Ajayaghosh, A.; George, S. J. *J. Am. Chem. Soc.* **2001**, *123*, 5148−5149. (b) Varghese, R.; George, S. J.; Ajayaghosh, A. *Chem. Commun.* **2005**, 593−595. (c) George, S. J.; Ajayaghosh, A. *Chem.-Eur. J.* **2005**, *11*, 3217−3227.
(24) (a) George, S. J.; Ajayaghosh, A.; Jonkheijm, P.; Schenning, A. P. H. J.; Meijer, E. W. *Angew. Chem. Int. Ed.* **2004**, *43*, 3422−3425. (b) Ajayaghosh, A.; Vijayakumar, C.; Varghese, R.; George, S. J. *Angew. Chem. Int. Ed.* **2006**, *45*. 456−459. (c) Ajayaghosh, A.; Varghese, R.; George, S. J.; Vijayakumar, C. *Angew. Chem., Int. Ed.* **2006**, *45*, 1141−1144.
(25) (a) Messmore, B. W.; Hulvat, J. F.; Sone, E. D.; Stupp, S. I. *J. Am. Chem. Soc.* **2004**, *126*, 14452−14458. (b) Hulvat, J. F.; Sofos, M.; Tajima, K.; Stupp, S. I. *J. Am. Chem. Soc.* **2005**, *127*, 366−372.
(26) Ajayaghosh, A.; George, S. J.; Praveen, V. K. *Angew. Chem., Int. Ed.* **2003**, *42*, 332−335.
(27) For a review on encapsulation of organic dyes see: Arunkumar, E.; Forbes, C. C.; Smith, B. D. *Eur. J. Org. Chem.* **2005**, 4051−4059.
(28) (a) Schenning, A. P. H. J.; Jonkheijm, P.; Peeters, E.; Meijer, E. W. *J. Am. Chem. Soc.* **2001**, *123*, 409−416. (b) Jonkheijm, P.; Hoeben, F. J. M.; Kleppinger, R.; van Herrikhuyzen, J.; Schenning, A. P. H. J.; Meijer, E. W. *J. Am. Chem. Soc.* **2003**, *125*, 15941−15949.
(29) See Supporting Information.
(30) Chrisstoffels, L. A. J.; Adronov, A.; Fréchet, J. M. J. *Angew. Chem., Int. Ed.* **2000**, *39*, 2163-2167.

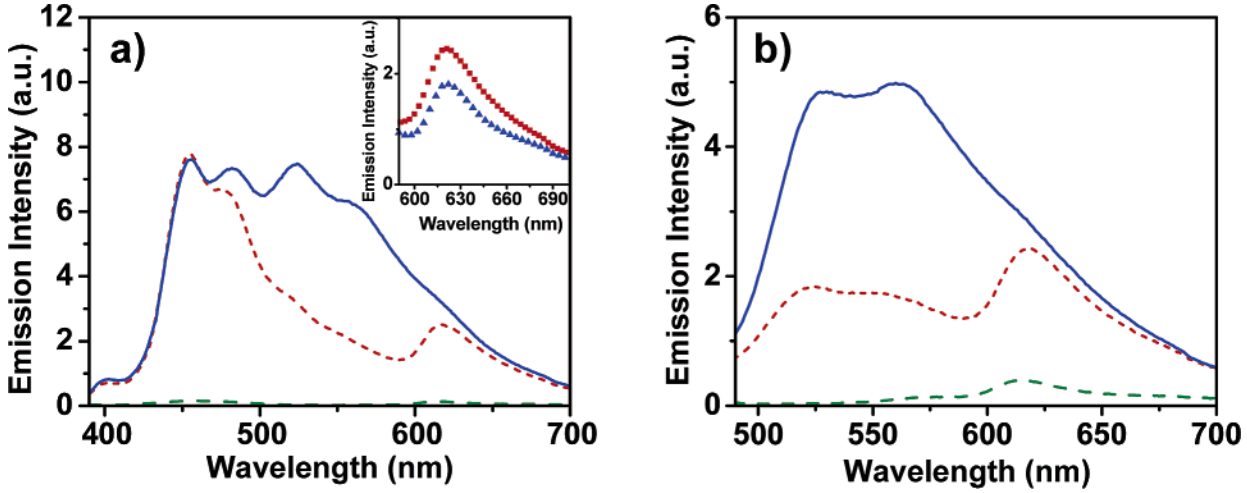

Figure 2. Emission spectra of **OPV1** (1.01×10^{-5} M) in the absence (blue ——) and in the presence (red - - -) of Rhodamine B (8.38×10^{-5} M). (a) In cyclohexane-chloroform (16:1) $\lambda_{ex} = 380$ nm. (b) Selective excitation of **OPV1** self-assembly at 470 nm in cyclohexane-chloroform (16:1). Emission of Rhodamine B (green — — —) in the absence of **OPV1**, on excitation at 380 nm is shown for a comparison. The inset shows the emission of the acceptor on indirect excitation at 470 nm (red ■) and direct excitation at 535 nm (blue ▲).

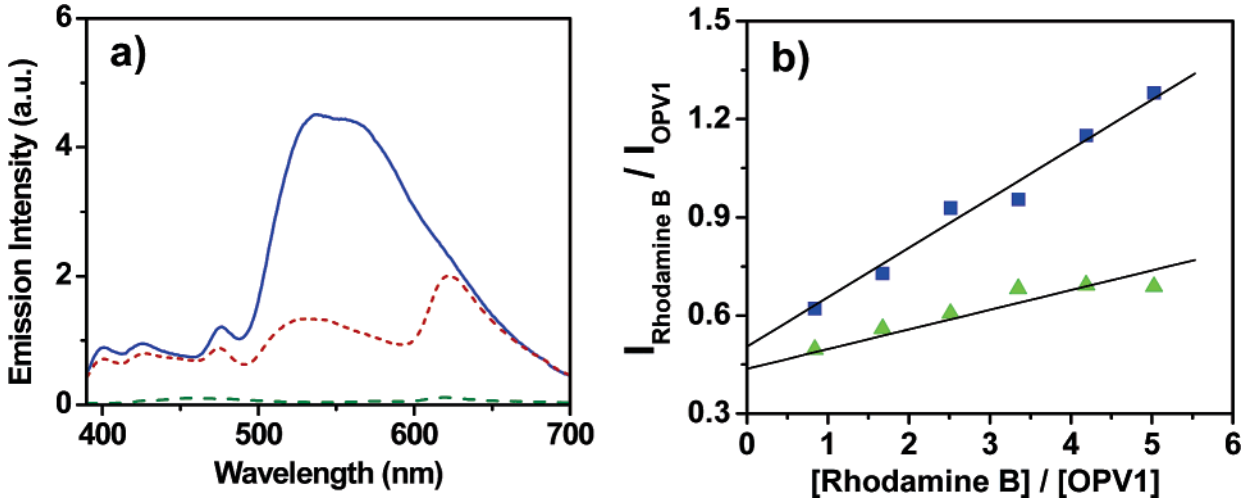

Figure 3. (a) Emission spectra of **OPV1** (1.01×10^{-5} M) in the absence (blue ——) and in the presence (red - - -) of Rhodamine B (8.38×10^{-5} M). The emission of Rhodamine B alone (green — — —) in dodecane-chloroform (16:1, $\lambda_{ex} = 380$ nm) is shown for a comparison. (b) Effect of solvents on the dependence of the relative fluorescence intensities against the molar ratio of the acceptor and the donor upon excitation at 380 nm. (blue ■) In dodecane-chloroform (16:1) and (green ▲) in cyclohexane-chloroform (16:1).

to the entrapped Rhodamine B is strongly influenced by the solvent used for inducing the self-assembly. For example, the emission spectrum of **OPV1** in dodecane-chloroform (16:1) is completely shifted toward the long wavelength region indicating efficient self-assembly of the molecules. Excitation at 380 nm in the presence of Rhodamine B showed nearly 72% quenching of the OPV emission (Figure 3a). Figure 3b shows the relative fluorescence intensity of Rhodamine B and **OPV1** when plotted against their molar ratio in dodecane-chloroform and in cyclohexane-chloroform, which showed an enhanced efficiency in the former case.

In the case of **OPV2**, which is a weakly aggregating molecule, the emission in cyclohexane and in dodecane revealed considerable difference when compared to those of **OPV1** (Table 1). In contrast to **OPV1**, **OPV2** in cyclohexane does not indicate considerable self-assembly of the molecules (Figure 4a). However, in dodecane the emission spectrum is considerably shifted toward long wavelength region indicating that majority of the molecule self-assembles in long chain hydrocarbon solvents (Figure 4b). Excitation of **OPV2** in the presence of Rhodamine B in cyclohexane-chloroform (16:1) shows a marginal quenching of the emission indicating that FRET is not efficient (ca. 10%) due to the weak self-assembly (Figure 4a). However, in dodecane-chloroform, the emission of **OPV2** is significantly quenched when excited at 380 nm (Figure 4b). A comparison of the relative emission of the acceptor and donor against the corresponding concentrations shows better FRET efficiency in dodecane-chloroform. Although **OPV2** showed considerable energy transfer to Rhodamine B (ca. 63%) in dodecane-chloroform (16:1), the efficiency was relatively low in cyclohexane-chloroform (16:1) when compared to that of the strongly self-assembling **OPV1** under identical conditions. These observations support the fact that the ability of the donor to form the self-assembly, which in turn is a solvent dependent process, is crucial for the efficient FRET.

Results of the FRET studies of **OPV3** with carboxylic end groups are shown in Figure 5. The presence of the two additional vinylic double bonds and the formation of the noncovalent polymeric assembly contribute to the shift and the broadening of the emission spectrum in hydrocarbon solvents. Addition of

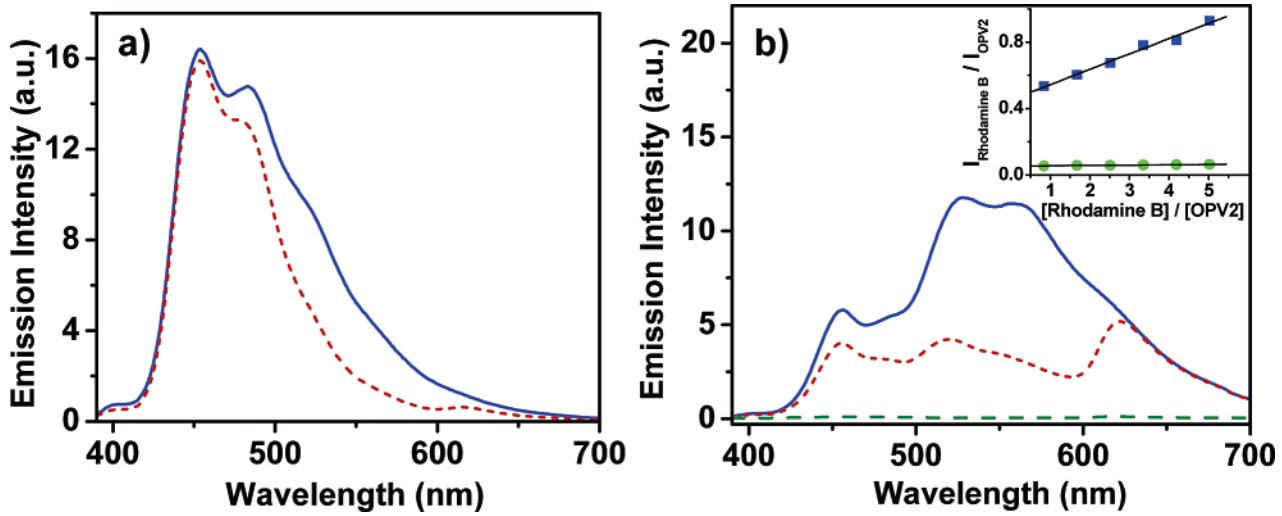

Figure 4. Emission spectra of **OPV2** (1.01×10^{-5} M) (a) in cyclohexane-chloroform (16:1) and (b) in dodecane-chloroform (16:1) in the absence (blue ——) and in the presence (red - - -) of Rhodamine B (8.38×10^{-5} M). Fluorescence of Rhodamine B (green — — —) in the absence of **OPV2** on excitation at 380 nm is also shown. Inset of (b) shows the effect of solvents on the dependence of relative fluorescence intensities of the acceptor and the donor against their molar ratio in cyclohexane: chloroform (green ●) and in dodecane-chloroform (blue ■).

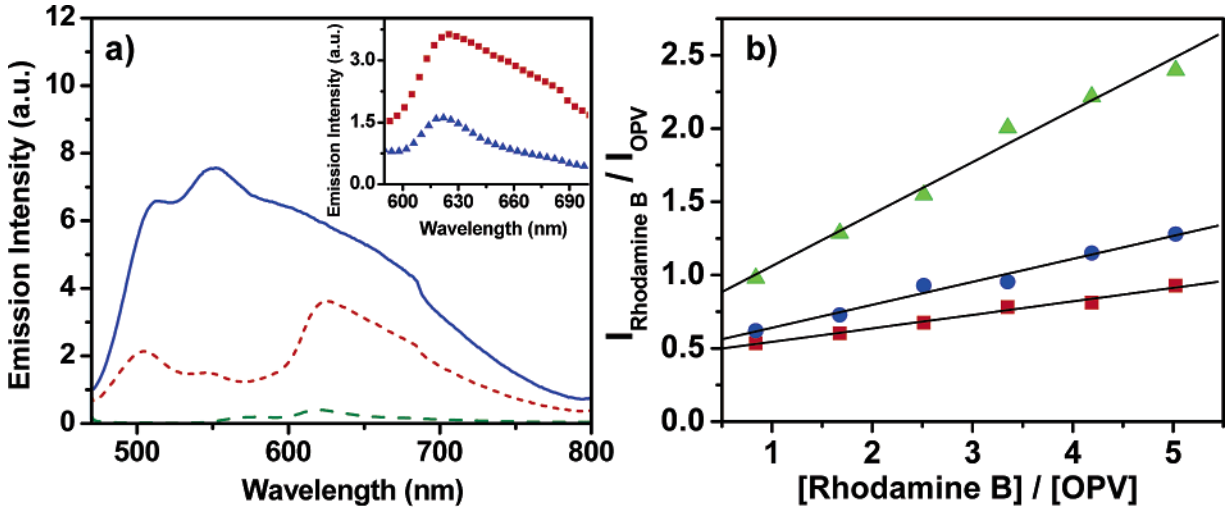

Figure 5. (a) Emission spectra of **OPV3** (1.01×10^{-5} M) in the absence (blue ——) and in the presence of Rhodamine B (4.19×10^{-5} M) (red - - -) in dodecane-chloroform (16:1). Fluorescence of Rhodamine B (green — — —) in the absence of **OPV3** ($\lambda_{ex} = 460$ nm) is shown for comparison. Inset of (a) shows the emission of the dye on indirect ($\lambda_{ex} = 460$ nm) (red ■) and direct excitation ($\lambda_{ex} = 535$ nm) (blue ▲). (b) Plots of relative fluorescence intensities against the molar ratio of the acceptor and the donor in dodecane-chloroform (16:1). **OPV1** (blue ●), **OPV2** (red ■), and **OPV3** (green ▲).

Rhodamine B into **OPV3** (1.01×10^{-5} M) in dodecane showed nearly 81% quenching of the fluorescence of the latter when excited at 460 nm. The concomitant formation of the Rhodamine B emission at 625 nm gets saturated at 4.19×10^{-5} M concentration of the acceptor (Figure 5a). Excitation of Rhodamine B alone at the same wavelength did not show significant emission. Comparison of the Rhodamine emission upon direct excitation at 535 nm and indirect excitation at 460 nm in the presence of **OPV3**, indicates that the FRET emission is nearly three times more intense than that of the emission from direct excitation. Noticeably, in this case four times excess of the acceptor is sufficient for the maximum quenching of the self-assembly emission in place of the eight times excess in the case of **OPV1**. Comparison of the relative fluorescence intensities of Rhodamine B with different OPVs against the respective molar ratios revealed maximum FRET efficiency for **OPV3** (Figure 5b). The better FRET efficiency of **OPV3** with relatively less amount of the acceptor indicates a better interaction of the former with the latter when compared to the results of **OPV1** and **OPV2**.

A unique feature of the present system is the thermal control on the FRET process. This is clear from the temperature-dependent emission changes of **OPV1** in the absence and in the presence of Rhodamine B (Figure 6). When cooled from 60 to 20 °C in dodecane-chloroform (16:1) the intensity of the emission maximum of **OPV1** at 452 nm is decreased and shifted to the region of 530−570 nm due to the self-assembly of the molecules (Figure 6a). However, while cooling from 55 to 20 °C in the presence of Rhodamine B, the emission maximum of **OPV1** is directly gated toward 625 nm, bypassing the emission of the self-assembled species at 530−570 nm (Figure 6b). Since the energy transfer between the donor and acceptor is usually independent of temperature, the observed thermal gating of FRET emission is the result of the thermoreversible breaking and making of the self-assembly which in turn thermally

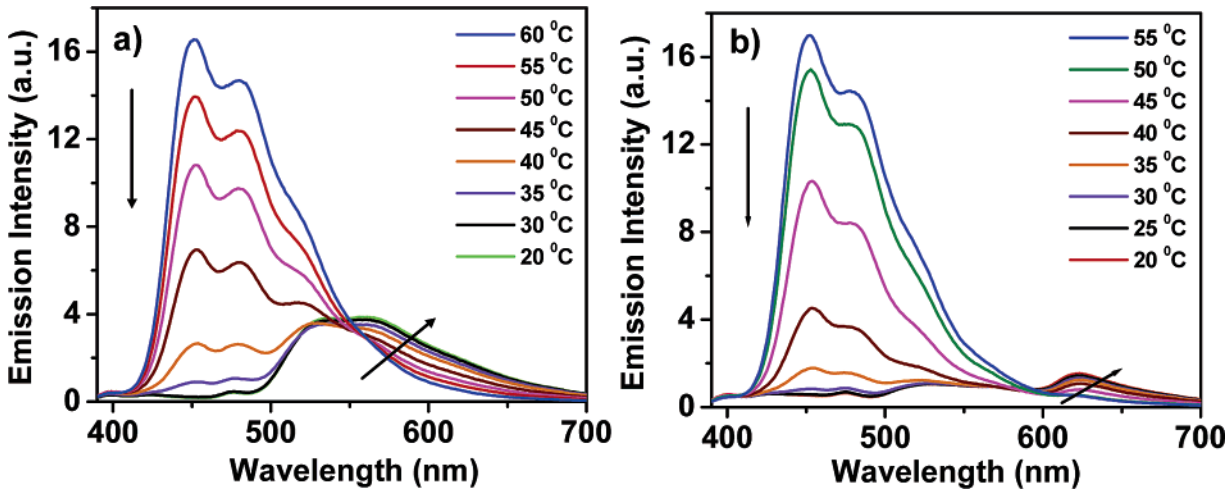

Figure 6. Temperature-dependent emission spectra of **OPV1** (1.01×10^{-5} M) (a) in the absence and (b) in the presence of Rhodamine B (8.38×10^{-5} M) in dodecane-chloroform (16:1). The weak emission of the self-assembly around 500−600 nm in (b) indicates the thermally gated energy transfer to Rhodamine B.

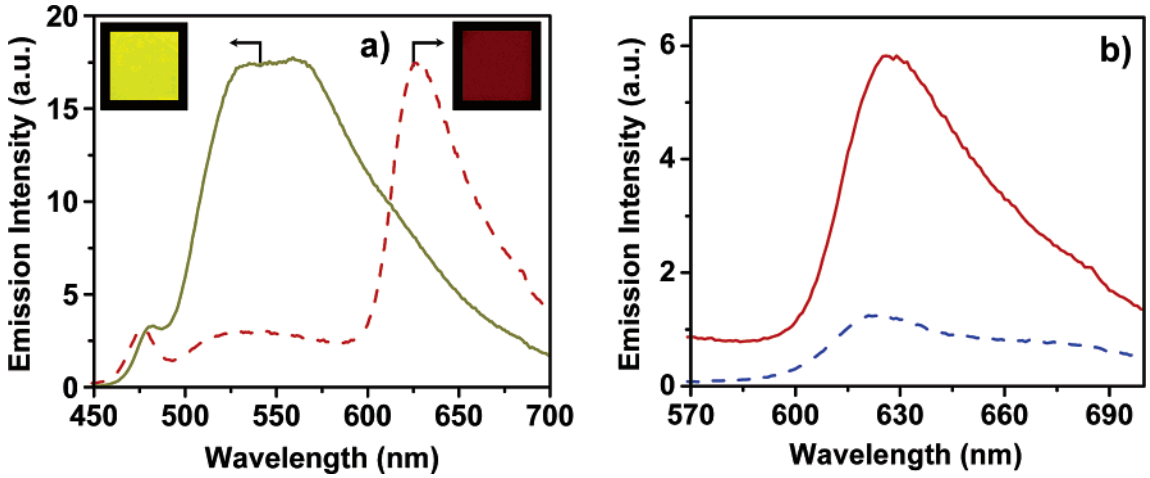

Figure 7. (a) Emission from the xerogel film of **OPV1** in the absence (greenish yellow ——) and in the presence of Rhodamine B (red − − −) (33 mol %) upon excitation at 380 nm. Emission colors of **OPV1** and **OPV1**+Rhodamine B films under UV light (365 nm) are shown in the inset of (a). (b) Comparison of the emission of Rhodamine B (red ——) at indirect excitation (380 nm) and direct excitation at 535 nm (blue − − −).

modulate the spectral overlap of the donor and the acceptor. Similar observation is made in the case of the temperature-dependent FRET studies of **OPV3**. In this case, although the molecularly dissolved **OPV3** emission matches with the absorption of Rhodamine B no evidence for FRET could be seen at higher temperature as inferred from the almost identical fluorescence intensities of the donor at same concentrations, in the absence and in the presence of the acceptor.[29] This observation highlights the importance of the supramolecular organization of chromophores in facilitating the FRET process.

One of the major limitations of the present system is the noncompatibility of the cationic acceptor with the OPV self-assembly in nonpolar solvents. Therefore, the major portion of the acceptor gets aggregated, which is not in contact with the bulk of the gel matrix. Moreover, the emission of the aggregated acceptor is very weak when compared to that of the monomer. Therefore, the intensity of the FRET emission of Rhodamine B in OPV self-assembly from dodecane or cyclohexane is weak. However, this problem could be solved partially by performing the FRET experiments in xerogel films. In the xerogel film the **OPV1** emission is completely shifted to the long wavelength region around 530 and 560 nm, corresponding to the self-assembled species (Figure 7a). Upon excitation of a Rhodamine B dispersed xerogel film of **OPV1** (1:2 molar ratio, 33 mol% of the acceptor) at 380 nm, the emission at 530−560 nm is almost completely quenched and the emission of the dye at 625 nm could be observed (Figure 7a). In this case, the intensity of the acceptor emission at 625 nm is enhanced nearly 6-fold when compared to that on direct excitation at 535 nm even though the dye concentration is only 33 mol% (Figure 7b). The insets of Figure 7a show the emission colors of the self-assembled **OPV1** film in the absence (greenish yellow) and in the presence (red) of Rhodamine B.

In light of the above observations, it is important to have insights into the morphology of the OPVs in the absence and in the presence of Rhodamine B. Scanning electron microscope (SEM) analysis reveals the initial formation of phase separated nanoaggregates of the acceptor when loaded in small amounts in the gel state of **OPV1** in cyclohexane (Figure 8b). A drop cast film in the presence of Rhodamine B from cyclohexane-chloroform reveals that the acceptor is uniformly aggregated around the supramolecular tapes (Figure 8c). The atomic force microscope (AFM) analysis of **OPV1** indicates the formation of supramolecular tapes of 5−15 nm thickness with 36−176

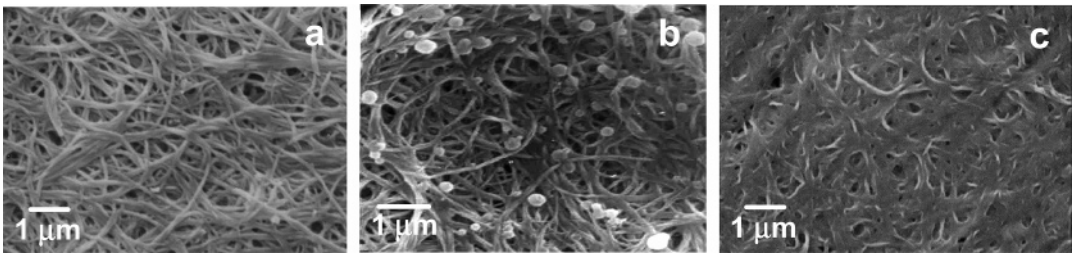

Figure 8. SEM pictures of **OPV1**. (a) Gel in cyclohexane, (b) gel in the presence of Rhodamine B and (c) a drop cast film in the presence of Rhodamine B.

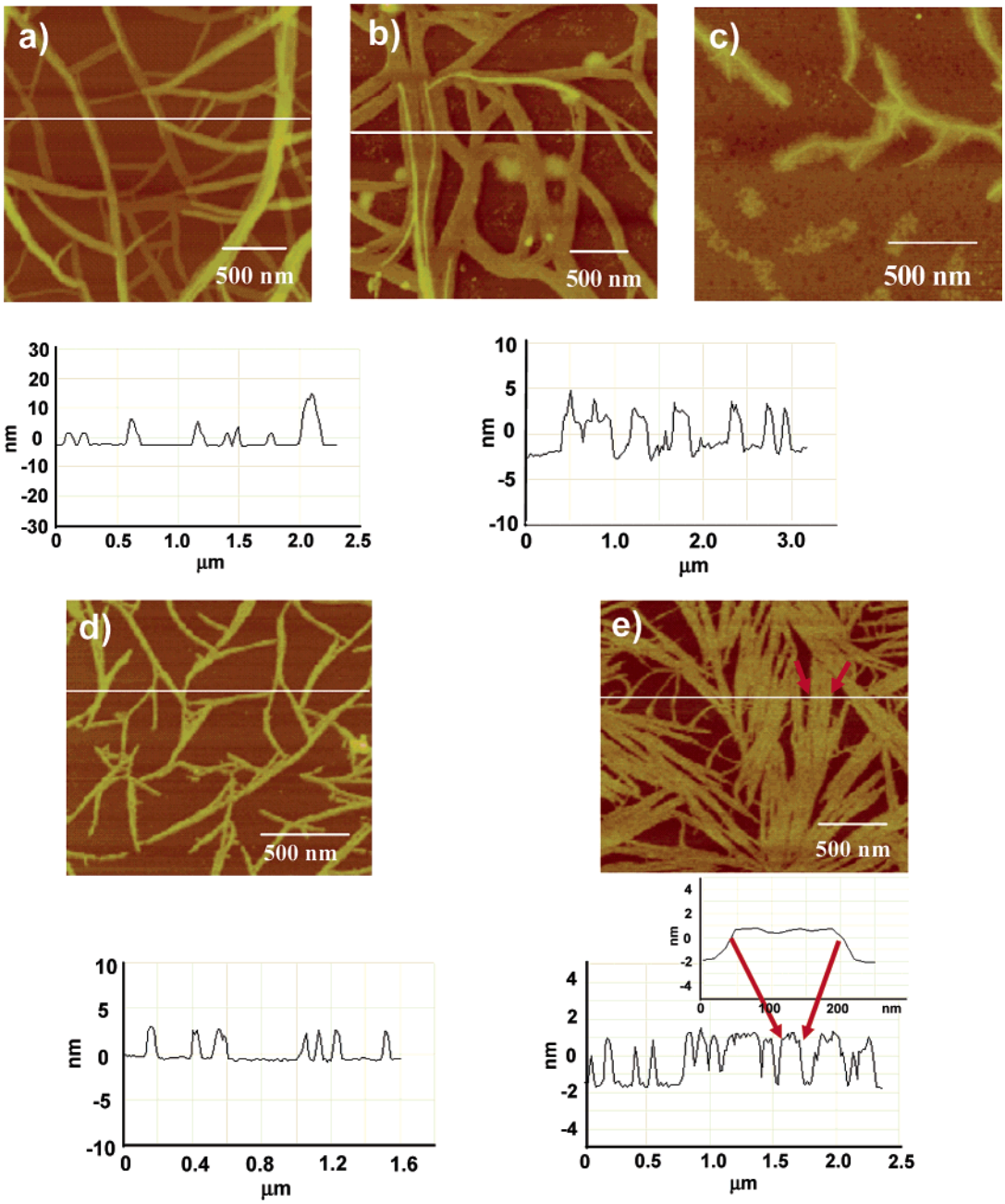

Figure 9. AFM taping mode height images and the corresponding section analysis of (a) **OPV1,** (b and c) **OPV1** + Rhodamine B, (d) **OPV3** and (e) **OPV3** + Rhodamine B. The section analyses of images a, b, d, and e are also shown. In all experiments [OPV] = 5×10^{-5} M and [Rhodamine B] = 2×10^{-4} M. Blank experiments were performed with solvent alone to rule out any artifacts. Samples were prepared by drop casting the dodecane-chloroform (16:1) solution of the compound onto a freshly cleaved, mica surface. The actual size of the self-assemblies were estimated by subtracting the tip broadening factor from the measured size.[31]

(±10) nm width and several micrometers in length (Figure 9a). Addition of Rhodamine B indicates the localization of the latter around the tapes (Figure 9b). In addition the phase separated aggregates of the dye is also seen in the AFM picture (Figure

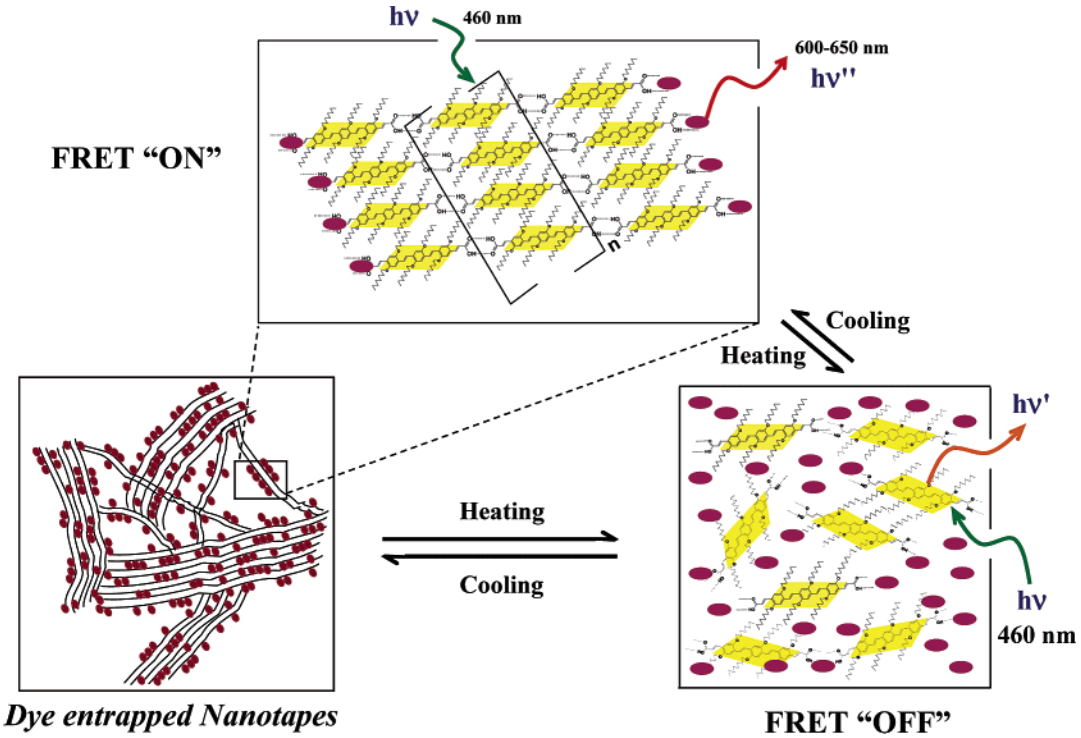

Figure 10. Cartoon representation of the self-assembly induced FRET from **OPV3** to Rhodamine B.

9c). Interestingly, **OPV3** showed the formation of interconnected short linear tapes of 1−2 μm in length, 54−84 ($\pm$1) nm in width and 3 $\pm$ 0.5 nm in height (Figure 9d). These structures are considerably different from those of the entangled nanotapes of **OPV1**. The AFM pictures reveal that in the presence of Rhodamine dye, individual fibers of **OPV3** are agglomerated along the edge as seen in Figure 9e. Interestingly, the AFM height profiles reveal that the thickness and the width of the individual tapes do not vary considerably before and after the addition of the dye. This means that the presence of the dye does not disturb the original morphology of the OPVs, rather the aggregated dye tend to localize on the polar edges of the tapes.

On the basis of the morphological analysis, the plausible arrangement of the Rhodamine dye entrapped OPV self-assembly is shown in Figure 10. The two edges along the axis of the self-assembled OPV tapes are polar due to free carboxylic acid or hydroxyl groups on which the Rhodamine dye is localized. This is clear from the AFM pictures which reveal that most of the dye molecules are aggregated between tapes when the solvent is dried off before the image analysis. The energy transfer occurs preferably to the dye aggregates which are in contact with the self-assembled tapes. This could be the reason that an excess amount of the dye is needed for efficient quenching of the self-assembled OPV emission in cyclohexane and dodecane gel. However, in the case of the dye doped xerogel film, the dye molecules are in close contact with the OPV nanotapes, which could be within the Förster radii. This could be the reason for the enhanced efficiency of FRET in the case of the self-assembled film, even at low dye concentrations when compared to that in the organogel state. We are currently working toward increasing the efficiency of energy transfer with the help of suitable acceptors which are compatible with the OPV gel matrix, and these results will be published in near future.

Conclusions

We have demonstrated the use of self-assembled OPV nanotapes as donor scaffolds to achieve thermally gated FRET to entrapped Rhodamine B. The FRET efficiency depends on the ability of the OPVs to form self-assemblies which is strongly influenced by the end functional groups as well as the solvent. The edges of the H-bonded nanotapes are polar due to the presence of free $-CO_2H$ or $-OH$ groups where the acceptor molecules are preferably localized. FRET occurs exclusively from the self-assembled OPVs to the physically attached acceptors and not from the individual donor molecules. More importantly, since FRET occurs exclusively from the self-assembled molecules, it could be thermally controlled by the reversible self-assembly process. FRET is found to be more efficient in a xerogel film when compared to that of the self-assembly in dodecane or cyclohexane gel. This is a unique example of nanostructured π-conjugated self-assemblies as energy donor scaffolds for thermally gated FRET processes and could be an entry to a novel class of functional supramolecular materials.

Experimental Section

General. Unless otherwise stated, all starting materials and reagents were purchased from commercial suppliers and used without further purification. The solvents used were purified and dried by standard methods prior to use. Melting points were determined with a Mel-Temp-II melting point apparatus and are uncorrected. ^{1}H and ^{13}C NMR spectra were measured on a 300 MHz Bruker Avance DPX spectrometer using TMS as internal standard. FT-IR spectra were recorded on a Shimadzu IRPrestige-21 Fourier Transform Infrared spectrophotometer. Matrix-assisted laser desorption ionization time-of-flight (MALDI-TOF) mass spectra were obtained on a Perseptive Biosystems Voyager DE-Pro MALDI-TOF mass spectrometer using α-Cyano-4-hydroxy cinnamic acid as the matrix.

FRET Studies. Energy transfer experiments were carried out in cyclohexane-chloroform or dodecane-chloroform solvent mixtures (16:

1). Samples for the FRET studies were prepared by adding appropriate concentration of the dye in 0.2 mL chloroform to 3 mL cyclohexane or dodecane solution of OPVs. Energy transfer studies in the film form was performed by drop casting a film of the appropriate OPV containing 10−33 mol% of Rhodamine B from cyclohexane-chloroform. The film was dried in a vacuum oven before recording the emission spectra.

The efficiency of energy transfer was estimated from the donor fluorescence quenching profiles by using the eq 1.[32]

$$\text{efficiency of energy transfer} = 1 - \frac{I_{DA}}{I_D} \qquad (1)$$

where I_D and I_{DA} are emission intensities of the donor in the absence and presence of acceptor, respectively.

Preparation of 3. To a solution of the bisaldehyde **1** (0.56 mmol) and the phosphonate **2** (1.12 mmol), in 35 mL THF, NaH (3.7 mmol) was carefully added under argon atmosphere. The reaction mixture was refluxed for 8 h, and the solvent was removed under reduced pressure. The resultant residue was extracted with chloroform and washed several times with saturated brine and water. Concentration of the organic layer followed by column chromatography (hexane/chloroform, 3:1) over silica gel (100−200 mesh) gave the pure **3** as an orange solid. Yield-71%; mp 97−99 °C; FT-IR (KBr): ν_{max} 668, 860, 963, 1082, 1175, 1212, 1253, 1351, 1424, 1475, 1506, 1600, 1636, 1724, 2856, 2934 cm^{-1}; ^1H NMR (300 MHz, $CDCl_3$, TMS) δ 0.85−0.89 (t, 18H, $-CH_3$), 1.24−1.86 (m, 174H, $-CH_2-$), 3.97−4.07 (m, 12H, $-OCH_2-$), 4.23−4.30 (q, 4H, $-COOCH_2-$), 6.48−6.54 (d, J = 16.09 Hz, 2H, Vinylic), 7.03 (s, 2H, aromatic), 7.14 (s, 4H, aromatic), 7.43−7.49 (d, J = 16.62 Hz, 2H, Vinylic), 7.51−7.56 (d, J = 16.41 Hz, 2H, Vinylic), 7.96−8.01 (d, J = 16.09 Hz, 2H, Vinylic) ppm;^{13}C NMR ($CDCl_3$, 75 MHz) δ 14.12, 14.36, 22.69, 26.21, 26.30, 29.38, 29.47, 29.53, 29.67, 29.72, 31.92, 60.28, 69.20, 69.39, 110.09, 110.60, 112.31, 117.86, 123.19, 124.93, 127.38, 130.52, 139.74, 150.62, 151.17, 152.49, 167.58 ppm; MALDI−TOF MS (MW = 1921.13): m/z = 1921.88 $[M]^+$.

Preparation of OPV3. KOH (5 N) in methanol (40 mL) was added to a solution of the diester **3** (0.75 mmol) in THF (50 mL). The reaction mixture was refluxed at 70 °C for 4 h. The solvent was then evaporated, and the residue was suspended in THF (50 mL). Trifluoroacetic acid was added to adjust the pH around 2. The solvent was then evaporated, and the solid residue was washed with cold water until the washings stayed neutral. Finally, the solid was washed with cold (ice bath) THF and dried in a vacuum oven to get **OPV3** as a red solid. Yield-93%; mp 203−205 °C; FT-IR (KBr): ν_{max} 725, 855, 1046, 1206, 1258, 1429, 1470, 1506, 1594, 1625, 1687, 2856, 2924, 3441 cm^{-1}; ^1H NMR (300 MHz, $CDCl_3$, TMS) δ 0.80−0.83 (t, 18H, $-CH_3$), 1.17−1.79 (m, 168H, $-CH_2-$), 3.96−4.08 (m, 12H, $-OCH_2-$), 6.43−6.48 (d, J = 15.07 Hz, 2H, Vinylic), 6.96 (s, 2H, aromatic), 7.08 (s, 4H, aromatic), 7.36−7.42 (d, J = 16.01 Hz, 2H, Vinylic), 7.45−7.5 (d, J = 16.11 Hz, 2H, Vinylic), 7.97−8.02 (d, J = 15.09 Hz, 2H, Vinylic) ppm;^{13}C NMR (d_8-THF, 75 MHz) δ 13.6, 14.21, 22.71, 26.31, 28.41, 29.42, 29.53, 29.67, 29.92, 31.42, 59.28, 70.20, 71.32, 111.09, 112.60, 113.31, 119.86, 122.19, 123.82, 125.92, 128.32, 130.51, 140.01, 151.07, 152.11, 153.19, 167.49 ppm; MALDI-TOF−MS (MW = 1865.02): m/z = 1865.31 $[M]^+$.

Acknowledgment. We thank Mr. Prabhakar Rao for SEM analysis. This work (Manuscript No. RRLT-PRU 221) is supported by the Department of Science and Technology (DST), Government of India, New Delhi and CSIR Task Force Program (CMM 010). V.K.P., S.J.G., R.V., and C.V. thank the CSIR for research fellowships.

Supporting Information Available: General description of the spectroscopic and microscopic techniques, optical properties of **OPV3**, overlap spectra of **OPV1-3** with Rhodamine B, temperature-dependent emission spectra of **OPV3** in the absence and presence of Rhodamine B. This material is available free of charge via the Internet at http://pubs.acs.org.

JA0587594

(31) The image broadening due to the AFM tip convolution effect is estimated as reported in: Samori, P.; Francke, V.; Mangel, T.; Müllen, K.; Rabe, J. P. *Opt. Mater.* **1998**, *9*, 390−393. The radius of the tips (Veeco probes, MPP-11100−10) is taken as 12.5 nm. For **OPV1**, the measured height of the tapes is 5−15 nm and the calculated tip broadening is 24 ± 10 nm. Therefore, the actual width of the tapes is estimated by subtracting the broadening factor from the measured width (60−200 nm) which is 36−176 ± 10 nm. Similarly, for **OPV3** the apparent height of the tapes is 3 ± 0.5 nm and the calculated tip broadening is 16 ± 1 nm, hence the actual width is 54−84 (± 1) nm.

(32) Lakowicz, J. R. *Principles of Fluorescence Spectroscopy*, 2nd ed.; Kluwer Academic/Plenum Publishers: New York, 1999.